

### **3.1 Introduction**

Promising nanomaterials which have been emerged from the recent past by many experimental and theoretical groups are boron nitride nanostructures (BNNs) which include nanotube, nanoribbon and nanosheet [1-4]. They are one of the most reliable materials for the utilization in medical applications, bio sensing, nano electronics and drug delivery because of its exceptional properties like oxidation resistance, high temperature stability, large thermal conductivity and low dielectric constant [5-10]. Boron nitride exists in cubic BN (c-BN), trigonal BN, wurtzite BN (w-BN) and hexagonal BN (h-BN) isomers. However, h-BN received maximum attention [11-12].

The polar character of BNNs provides an advantage over its carbon counterpart [13]. The nontoxicity and large intrinsic bandgap which are attributed due to its ionic bonding nature makes these nanomaterials more suitable for bio applications than its carbon counterpart [14]. The tuning of the band gap is easily achieved with boron nitride nanoribbon (BNNR), which is not the case with graphene nanoribbon (GNR) [15-16]. The BNNR has similar classified configuration as GNR: (a) zigzag BNNR (ZBNNR) and (b) armchair BNNR (ABNNR) [17-19]. Many studies exist in the literature about the diverse properties of both ribbons [18-20], like monotonous decrement in the bandgap for ZBNNR with increase in width while in case of ABNNR there is an oscillatory bandgap with increasing in ribbon width [21]. The non-cytotoxicity of BNNs resulted in many experimental and theoretical studies on their interaction with several biomolecules [22-25]. There exist many studies which report

modulation in the biocompatibility of these BNNs useful for biological and medical applications [26-29].

Two of the important members in alkaloid family are caffeine and nicotine which are used as therapeutic molecules in medical purposes [30-31] mainly obtained from coffee and tobacco. These molecules serve as stimulants for central nervous system in human body. Caffeine is a methylxanthine and has the most notable pharmacological effect in human body like central nervous system stimulation, increasing alertness and producing agitation. The modulation of intracellular calcium handling is one of the most important uses of caffeine. The nicotine mainly obtained from tobacco plant have tendency to acts as an agonist at the nicotinic receptors at neuromuscular junctions in the adrenal medulla and the brain. As both of them are therapeutic drugs, they show positive effect if consumed in proper quantity on human but can be calamitous for heavy consumption. High consumption can cause severe side effects like insomnia, high heart rate and high blood pressure [32]. Due to addictive nature of these drugs, many country bans on the sale and or production of many products which uses these molecules as a major ingredient mainly in energy drinks. Therefore, high sensitive sensors for them, based on nanostructures to sense and filter these biomolecules need to be improved. Recently, nanomaterials made up of carboxylate carbon nanotube (CNT) have been utilized as an addition in the filter tip of cigarettes to increase nicotine and tar sorption [33].

There are some reports bringing light on the interaction of nicotine molecule with CNT by using density functional theory (DFT) [34-35]. However different binding geometries and binding energies are reported in literature [34-35]. BNNT shows better chemical stability than its carbon counterpart CNT due to its resistance towards oxidation [36-38]. There exist many

studies on the interaction of caffeine and nicotine with boron nitride nanocage  $B_{12}N_{12}$  and  $B_{16}N_{16}$  [39] where a chemical interaction is observed between the molecules and nanocage with superior adsorption energy over  $B_{12}N_{12}$  cage for both caffeine and nicotine molecules. Over the interaction of HCN and methanol molecules with BN nanocage, modification in electrical conductance, binding energies and binding geometries is observed [40-41]. For understanding the nature of interaction and effect on the electronic transport by biomolecule like nucleobases and amino acids on BN nanostructures few studies are reported in literature [42-43]. However, in these studies authors have ignored the most important contribution of dispersion which is due to the weak vdW interactions. Adsorptions as well as electronic properties in boron nitrides nanostructures are highly dependent on arrangement of atoms, length and dimension. In the present work, we carried out a systematic study on the interaction of biomolecules; alkaloids with BN nanoribbons (BNNR) and BN nanotube (BNNT) and identify the factors influencing the interaction. Furthermore, we want to check the contribution of vdW in adsorption energy of alkaloids over boron nitride nanostructures by first principles based dispersion corrected density functional theory calculation.

### **3.2 Computational Methods**

All first-principle calculations in the present work were carried out using Quantum espresso code [44] which uses plane wave pseudopotential approach within the generalized gradient approximation (GGA) [45] exchange correlation functional. For the convergence of lattice parameters and total energy, the single particle function are developed in plane wave basis set with the kinetic energy cut off 80 Ry and charge density 800 Ry. The Brillouin zone

is sampled using 1x1x8 and 1x16x1 Monkhorst-Pack [46] for BNNT and BNNR respectively, after performing the convergence corresponding to **k**-point grids. For the structural optimization, all the considered systems are fully relaxed with the residual forces less than 0.001eV/Å. Through the study of full structural optimization, adsorption mechanism, electronic properties and density of states (DOS), a comparative analysis has been carried out with two alkaloids namely caffeine and nicotine interaction with BNNT and BNNR. The average bond length of B-N in pristine BNNT and BNNR after the optimization was found to be 1.48 Å. For the weakly bound systems, a dispersion force is required in order to attain an accurate quantum mechanical description between interactions of molecules with nano-surface [47]. Therefore, it is significant to select an appropriate computational method which gives correct description of long-range electron correlation. To include the long distance van der Waals in the interaction between the molecules and BNNs, present work includes Grimme's dispersion correction [48]. To analyze the adsorption mechanism, adsorption energies ( $E_{ad}$ ) are found through the equation:

$$E_{ad} = E_{BNN+alkaloid} - (E_{BNN} + E_{alkaloid}) \quad (3.1)$$

Where  $E_{BNN+alkaloid}$  is the total energy of BNNs (BNNT and BNNR) adsorbed by alkaloid (caffeine or nicotine),  $E_{BNN}$  is the total energy of the BNNT or BNNR nanostructure,  $E_{alkaloid}$  is the total energy of alkaloid (caffeine or nicotine) acquired from their fully optimized geometries. Moreover,  $E_{ad} < 0$  shows the exergonic character of the adsorption. We have also calculated the quantum conductance at zero bias using the Landauer formalism [49], through maximally localized Wannier functions (MLWF) basis in the Wannier90 code [50].

3.3 Results and Discussion

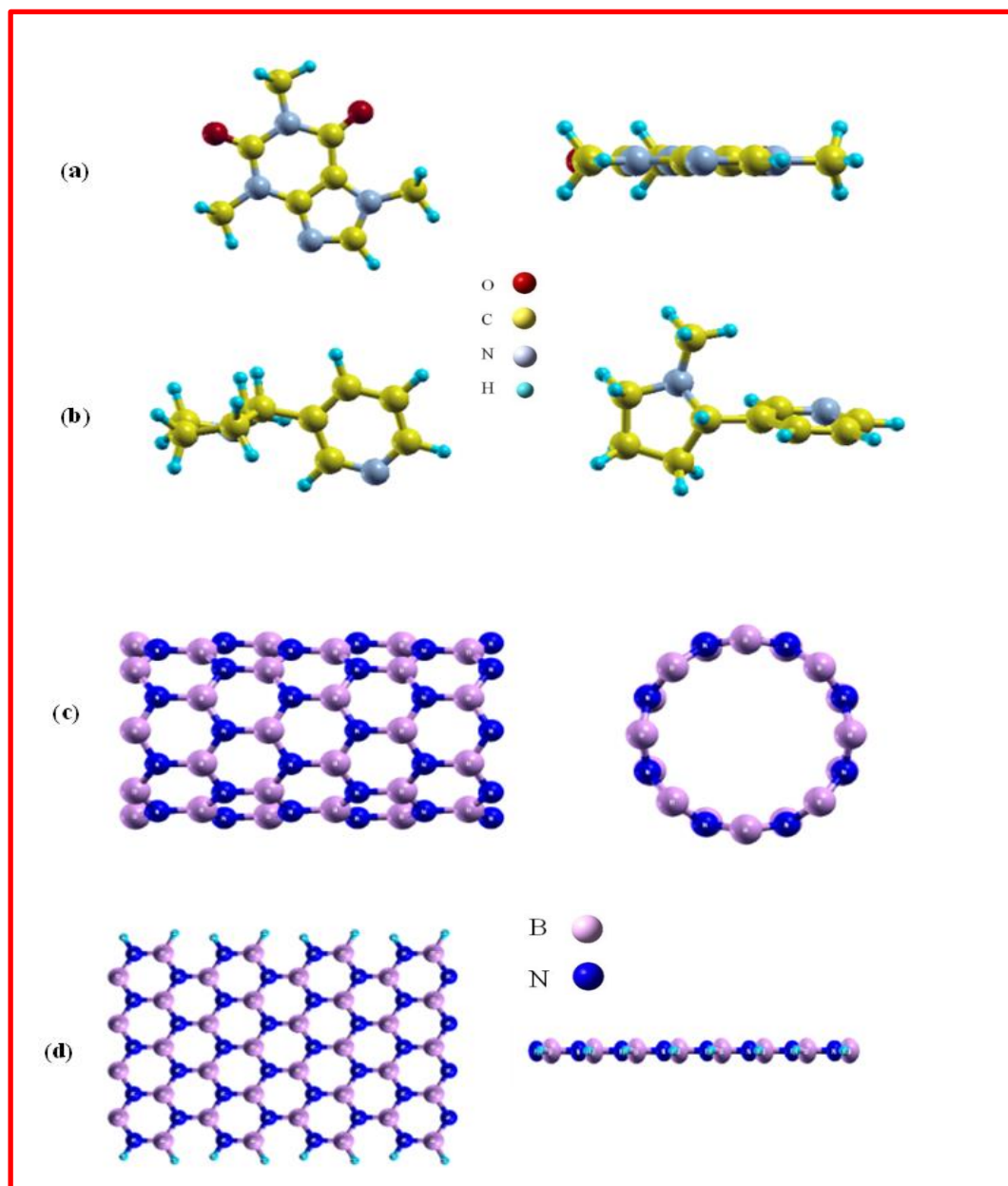


*Figure 3.1: Optimized structure of (a) caffeine (b) nicotine (c) pristine boron nitride nanotube and (d) pristine boron nitride nanoribbon. The figure also shows the side view of optimized structures.*

At first, we have performed full structural optimization of BNNT, BNNR, caffeine and nicotine for proper understanding of the interaction between alkaloids (caffeine and nicotine) and two boron nitride nanostructures (BNNs). All optimized structures are presented in Figs. 3.1(a-d). The optimized diameter of (8,0) BNNT and width of BNNR is found 6.40 Å and 10.03 Å respectively.

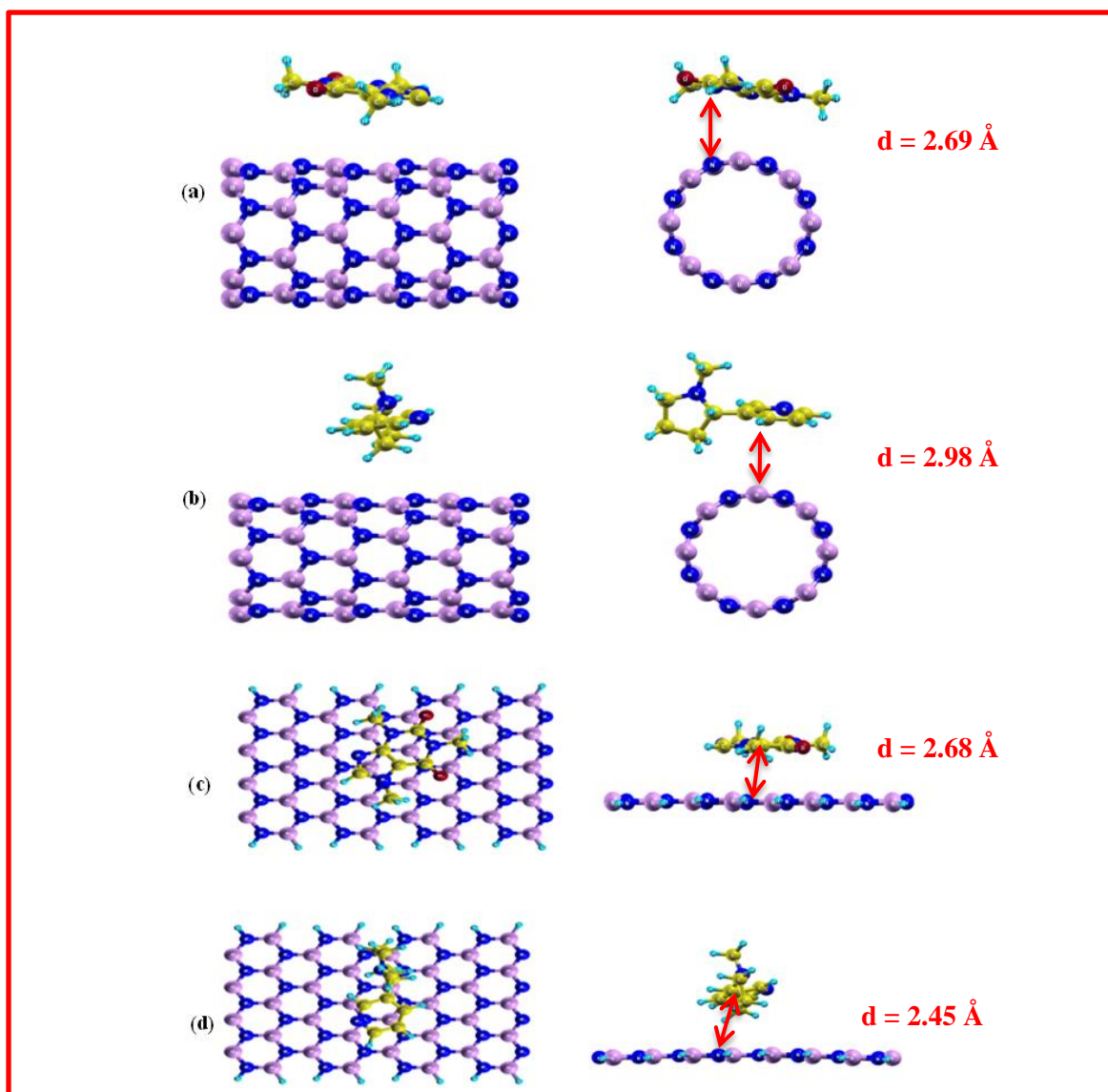


**Figure 3.2:** Equilibrium geometry of physisorbed caffeine and nicotine molecules on (a-b) BNNT and (c-d) BNNR. The figure also shows the side view of optimized structures of functionalized BN nanostructures with alkaloids.

**Table 3.1:** Calculated HOMO energies, LUMO energies, energy band gap ( $E_g$ ), adsorption energy ( $E_{ad}$ ), Fermi level energies ( $E_F$ ) and distance of the molecules over BNNT ( $d$ ).

System	HOMO (eV)	LUMO (eV)	$E_g$ (eV)	$E_{ad}$ (eV)	$E_f$ (eV)	$d$ (Å)	
Without Dispersion	BNNT	-4.4285	-0.8656	3.563	-	-2.647	-
	Caffeine	-5.2272	-1.7121	3.515	-	-3.469	-
	Nicotine	-4.9027	-1.5005	3.402	-	-3.201	-
	BNNT+ Caffeine	-3.6309	-0.5969	3.034	-0.030	-2.113	3.6
	BNNT+ Nicotine	-3.2974	-0.6331	2.664	-0.025	-1.965	2.99
With Dispersion	BNNT	-4.4310	-0.8671	3.5634	-	-2.649	-
	Caffeine	-5.2273	-1.7122	3.515	-	-3.469	-
	Nicotine	-4.9027	-1.5005	3.402	-	-3.201	-
	BNNT+ Caffeine	-3.6185	-0.6199	2.999	-0.76	-2.119	2.69
	BNNT+ Nicotine	-3.3442	-0.6264	2.718	-0.35	-1.985	2.98
	BNNR	-4.5328	0.0234	4.556	-	-3.726	-
	BNNR+ Caffeine	-3.8187	-0.3484	3.470	-0.91	-2.401	2.68
BNNR+ Nicotine	-3.5103	-0.1156	3.395	-0.48	-3.385	2.45	

Before concluding the best orientation and optimized distance of molecules over both BNNs, we have tried different orientations (perpendicular and parallel) of molecules and

distances between molecules and nanostructures for best optimized geometries. The optimized structures of molecules adsorb over BNNs are presented in Figs. 3.2(a-d). The calculated adsorption energy of molecule with BNNs in perpendicular orientation is found very weak; the reason behind this low adsorption is less number of atoms in molecule facing the BNNs. The maximum adsorption energy of caffeine and nicotine over BNNT are found at distance 2.69 Å and 2.98 Å respectively which start decreasing with increasing distance and become zero around 6 Å while it shows repulsive behavior when the distance is decreased beyond 2.69 Å and 2.98 Å.

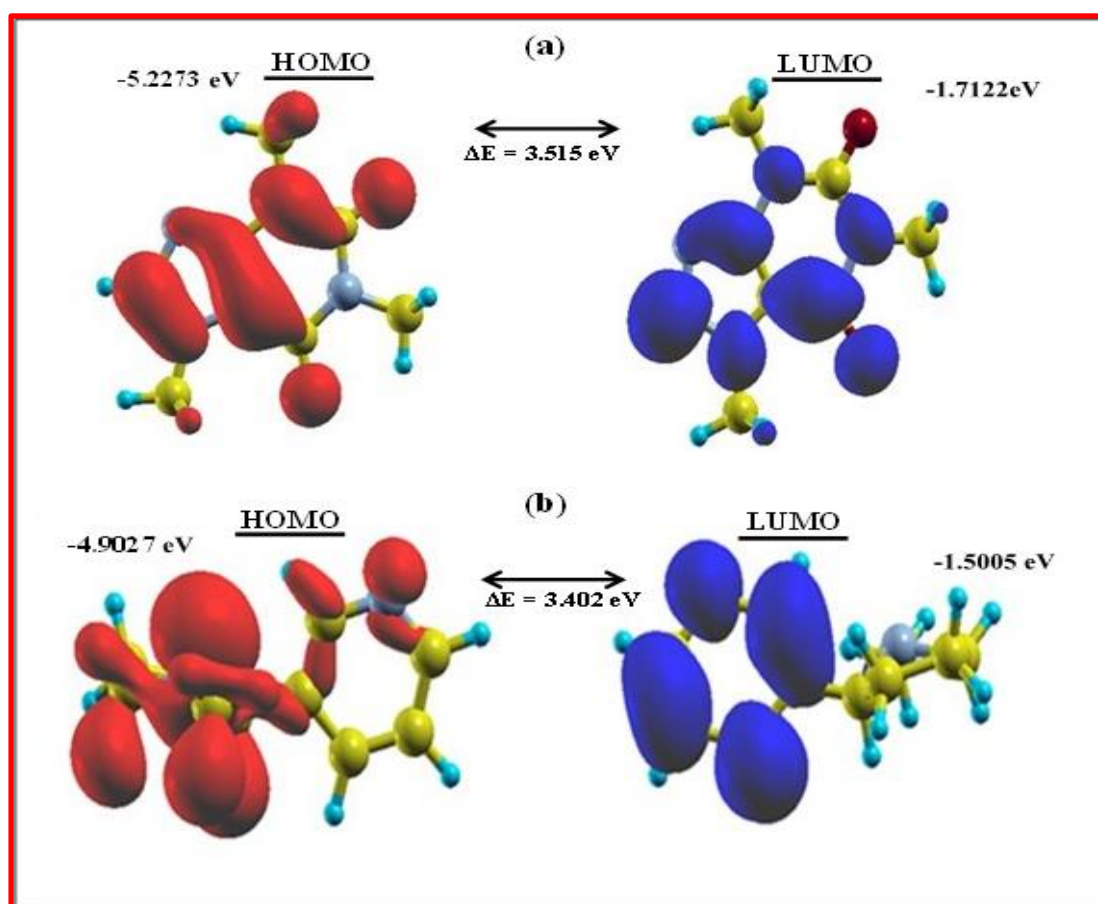


**Figure 3.3:** HOMO (red) and LUMO (blue) of (a) caffeine molecule and (b) nicotine molecule.

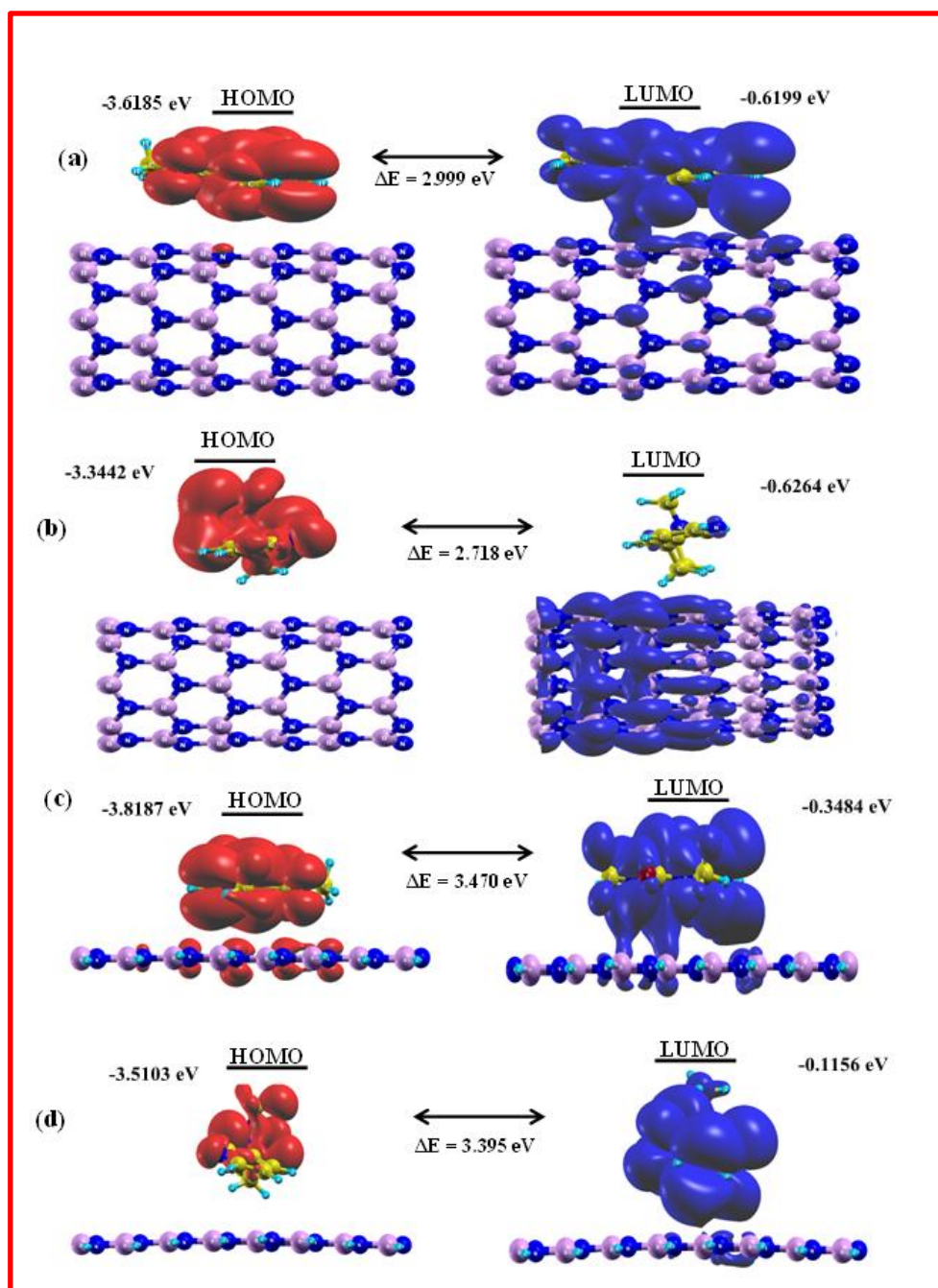


**Figure 3.4:** HOMO (red) and LUMO (blue) of functionalized BNNT (a-b) and BNNR (c-d) with caffeine molecule and nicotine molecule.

The most favorable orientation of caffeine and nicotine over BNNT and BNNR is

heteroatoms facing orientation for adsorption as can be clearly seen in the Fig. 3.2(b) that the nicotine molecule interact with its six member ring with BNNT rather than its five member ring similar to CNT [35]. In case of BNNR both rings of nicotine equally interact with the surface as large surface is available for interaction (Figs. 3.2(c-d)). All calculated values of energy gap ( $E_g$ ), HOMO and LUMO energies, adsorption energy ( $E_{ad}$ ), Fermi energy ( $E_f$ ) and distance ( $d$ ) between alkaloid molecules and BNNT/BNNR without and with dispersion corrections are presented in Table 3.1. Our calculated value of HOMO-LUMO gap for caffeine and nicotine molecules are in very good agreement with previously reported studies i.e. 3.515 eV and 3.402 eV respectively [35-39].

The HOMO and LUMO plots are presented in Figs. 3.3(a-b) of caffeine and nicotine and it can be seen from these figures that the wave functions are distributed over whole molecule in case of caffeine while in nicotine HOMO is dominating at five member ring and LUMO electron density is high at the phenyl group. The adsorbed alkaloids over BNNs significantly changes the HOMO and LUMO energy of BNNs as shown in Table 3.1, the calculated HOMO and LUMO are presented in Figs. 3.4(a-b) and Figs. 3.4(c-d) alkaloids/BNNT and alkaloids/BNNR systems respectively. The change in HOMO and LUMO energies is in the range of 0.71 to 1.0 eV and 0.35 to 0.48 eV after the adsorption of caffeine and nicotine over both BNNs respectively. The calculated charge density plots for caffeine and nicotine adsorbed BNNT and BNNR systems are presented in Figs. 3.5(a-b). We found that there is no significant charge transfer between alkaloids and BNNs as charges before and after adsorption of alkaloids on BNNs are less than 0.02e.

In both cases of alkaloids adsorption over BNNs, physisorption is observed as there is considerably large distance between the molecules and the surface (Table 3.1). After the inclusion of dispersion correction given by Grimme, which accounts the vdW interaction more precisely, significantly improves the adsorption energy of alkaloids over BNNs. Here we are presenting the results for BNNT with and without dispersion correction and not for BNNR as the results obtained for BNNT reveals the improvement in the adsorption energy with dispersion correction, therefore to save time we have done the calculation directly with the inclusion of dispersion in case of BNNR. As from the calculated values for adsorption energy presented in Table 3.1 we can see that the without dispersion correction we get quite low adsorption energy for alkaloids over BNNT. However, after the incorporation of dispersion corrections in DFT it properly accounts long range van der Waals interactions and correctly depict the adsorption energy. The adsorption energy calculation shows that the caffeine is strongly physisorbed over BNNT compared to nicotine because of lower adsorption energy. The caffeine and nicotine adsorption energies over BNNT are different due to  $\pi$  interaction of caffeine, which is almost double compared to nicotine similar to CNT [34-35].

The physical adsorption of nicotine is similar to previous study with CNT only until the CNT is defect free otherwise it gets covalently interacted at defected site [34]. From the results of adsorption energy calculation it is clear that BNNR has higher adsorption of alkaloids (caffeine and nicotine) showing dominance over BNNT. The calculated adsorption energies of alkaloids (caffeine and nicotine) over BNNR is -0.91 eV and -0.48eV respectively which are higher than BNNT which can be attributed to the fact that BNNRs are sensitive semiconducting in nature [11].

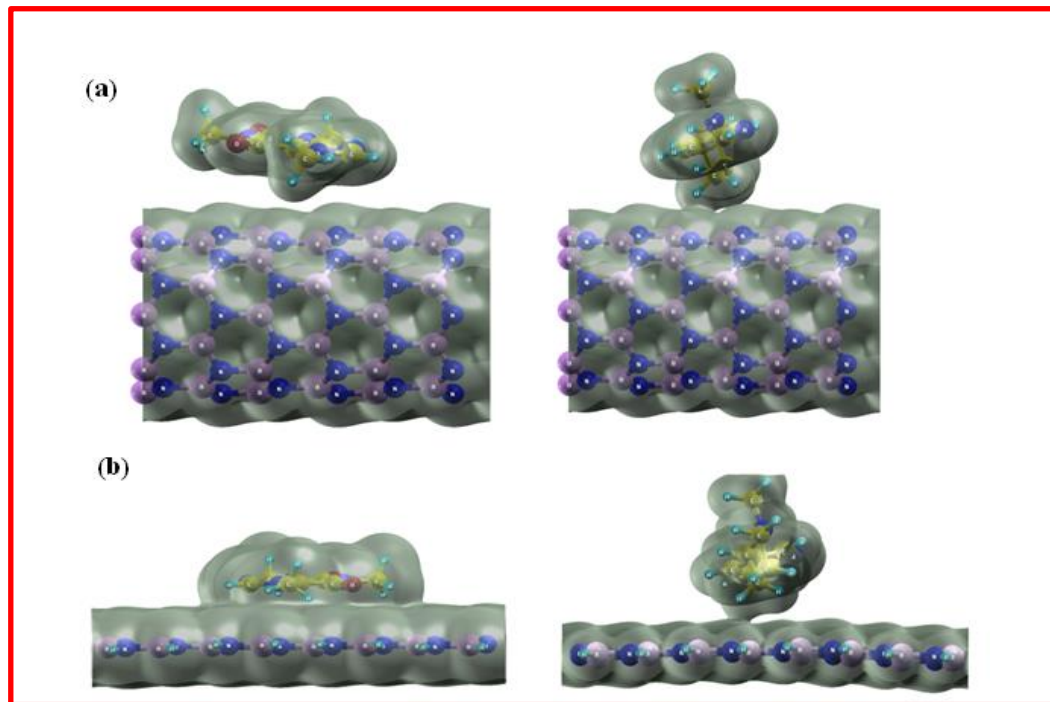


**Figure 3.5:** Total charge density plot of BNNT and BNNR conjugated with Caffeine and Nicotine (a) BNNT and (b) BNNR. Isosurface levels were set at  $0.09 \text{ bohr}^{-3}$ .

There can be seen significant effect on the adsorption distance of molecules over BNNs after the inclusion of vdW correction. The change is more in case of caffeine than nicotine which can be attributed to the fact of its planer structure providing large area for interaction [51-52]. There are some studies depicting the importance of inclusion of dispersion correction for calculating the adsorption energy of molecules over nanosurface. Study done by Dabbichi et al. [53] to understand the interaction of anthracene molecule over CNT after the inclusion of dispersion correction is found to have adsorption energy of 1 eV.

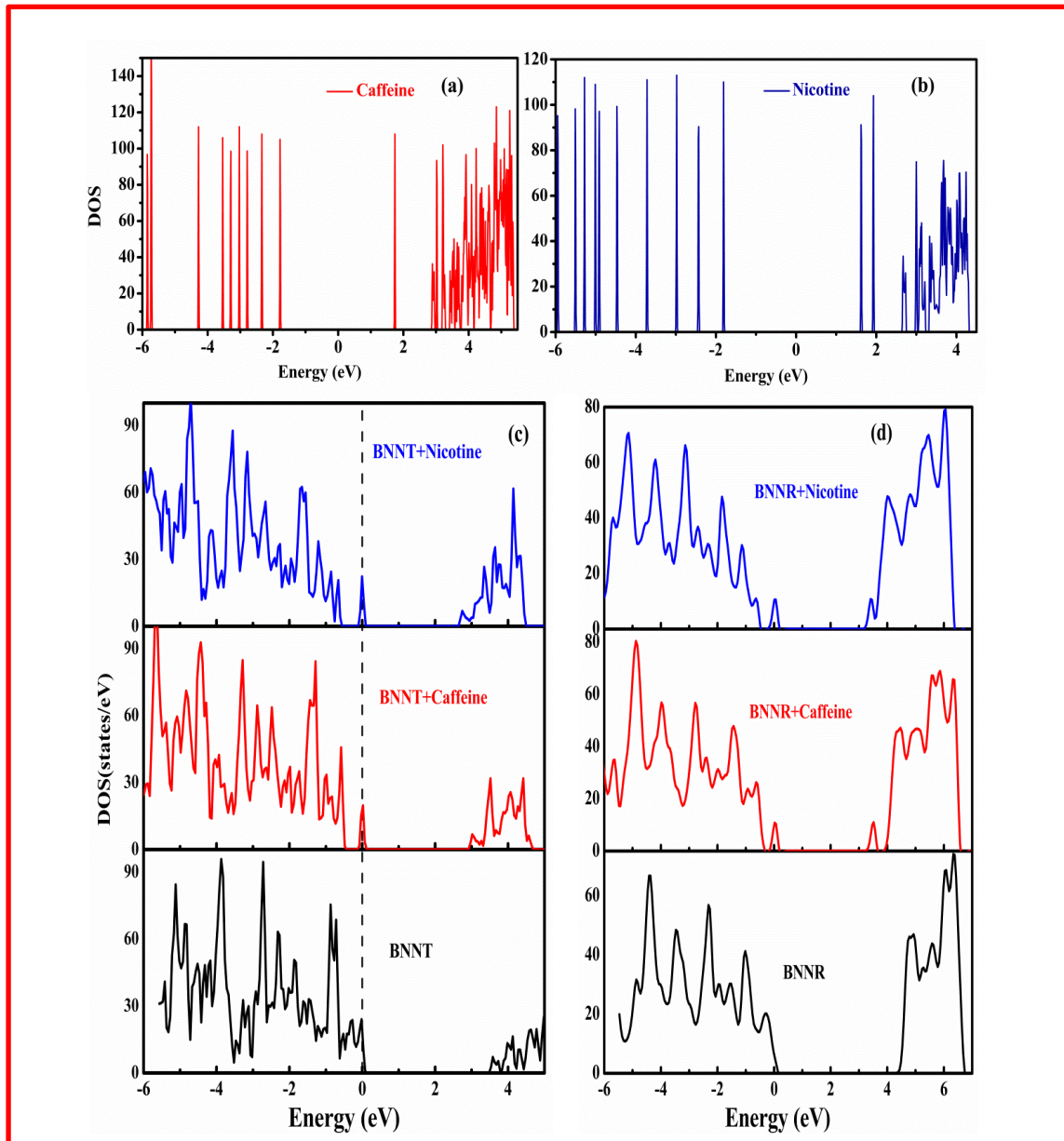


**Figure 3.6:** Total DOS of (a) caffeine molecule, (b) nicotine molecule, (c) pristine and alkaloid (nicotine and caffeine) conjugated BNNT and (d) pristine and alkaloid (nicotine and caffeine) conjugated BNNR.

Furthermore, study by Mukhopadhyay et al. [54] to check the interaction of five nucleobases with BNNT done with local density approximation (LDA) calculations pointed

out that the calculations done with LDA take care vdW forces and gives equivalent results as GGA + vdW level of theory gives. The difference in adsorption energy of these two alkaloids with the BNNT as well as BNNR is due to the van der Waals forces which are directly proportional to the size and mass of the interacting molecules [55]. All these observed results accentuate the role of van der Waals interactions in adsorption process. Any possibility of covalent bond between caffeine and nicotine molecules physisorbed over BNNT and BNNR are eliminated due to the large nearest atom distance ( $d \sim 2.6 \text{ \AA}$ ). The major advantage of physical adsorption on nanostructure is that it provides easy removal and reusability of nanostructure and also it does not affect structural or electronic properties of both adsorbate as well as adsorbent. Significantly better stable geometries are observed after optimization with the incorporation of dispersion correction. It was also seen that without the incorporation of dispersion correction, the calculated adsorption energy shows endergonic process, which means the interaction is not favorable electronically.

The BNNT and BNNR are more important in contrast to other BNNs for sensing purpose. For example our study reveals that the alkaloid molecules physisorbed over both BNNR/BNNT, which is key factor for any good as well as sensitive sensor because it reduces recovery time and increases response time [56]. But on the other hand, BN cage has chemisorption with the adsorbed molecule due to the ionic and covalent bonds between the molecule and the cage. The chemisorption process is normally irreversible and need external energy which causes increment in the recovery as well as response time, which is a major drawback for any sensor. To clearly understand the effect of alkaloids over BNNT/BNNR, we have done systematic calculation of total density of states (DOS) of caffeine, nicotine, BNNT,

BNNR and functionalized BNNT and BNNR with caffeine and nicotine in Figs. 3.6(a-d). For the better understanding of the orbital contribution in the electronic properties of BNNT/BNNR by alkaloid molecules we also calculated the projected DOS (PDOS) for both pristine BNNT and BNNR and the alkaloids (caffeine and nicotine) adsorbed BNNT and BNNR systems which are presented in Figs. 3.7(a-f).

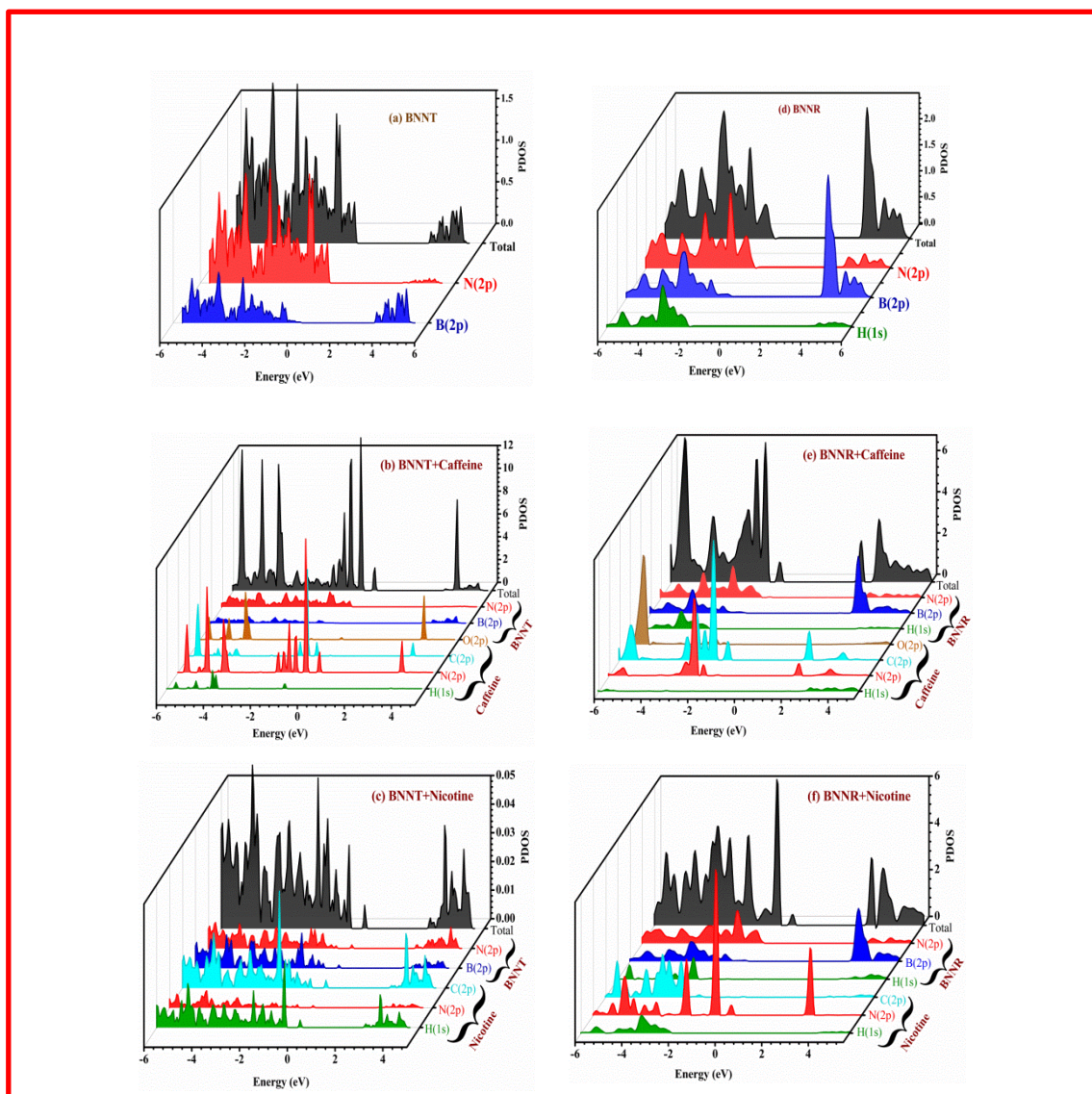


**Figure 3.7 :** PDOS of (a) pristine BNNT, (b) conjugated BNNT with caffeine, (c) conjugated BNNT with nicotine, (d) pristine BNNR, (e) conjugated BNNR with caffeine, (f) conjugated BNNR with nicotine.

From the figures it is clear that the alkaloid molecules significantly modulate the electronic properties of both BNNT and BNNR. The analysis shows that the major contributions of both molecule caffeine and nicotine are present in top of the valance band. The PDOS reveals that B(2p) and N(2p) orbitals have major contribution in the conduction and valance bands of both BNNT and BNNR (Figs. 3.7(a-f)) while N(2s) and B(2s) do not contribute significantly. The contribution of H(1s) can also be seen in the PDOS plots which is arising due to the edge passivation of BNNR. In pristine BNNT, HOMO states contribute mainly to the Fermi level compared to LUMO [54].

A significant feature resembling the molecule like spectra (sharp peaks) can be seen from DOS of both caffeine and nicotine molecules which arises due to the flat bands. In both molecules the value of the band gap is nearly equal. In case of BNNT adsorbed by alkaloids (Fig. 3.6(c)) conduction band region moves towards Fermi level while the valence band region shows a peculiar behavior. For BNNR adsorbed with caffeine and nicotine a large shift is observed away from Fermi level in the HOMO. There is a reduction in the band gap of both BNNs after the adsorption of caffeine and nicotine. Comparatively larger change in band gap is observed for BNNR than BNNT after adsorption of alkaloids. Hence, alkaloids act as an active unit which affects the mobility of electrons after adsorption on to the BNNs. Our adsorption energy calculations confirm physical adsorption for both caffeine and nicotine molecules over BNNT as well as BNNR. BNNR shows dominant adsorption of alkaloids than BNNT. Our results clearly depict that the BNNs are good candidate for biomedical applications because of its inert behavior as they do not affect the properties of carrier molecules.

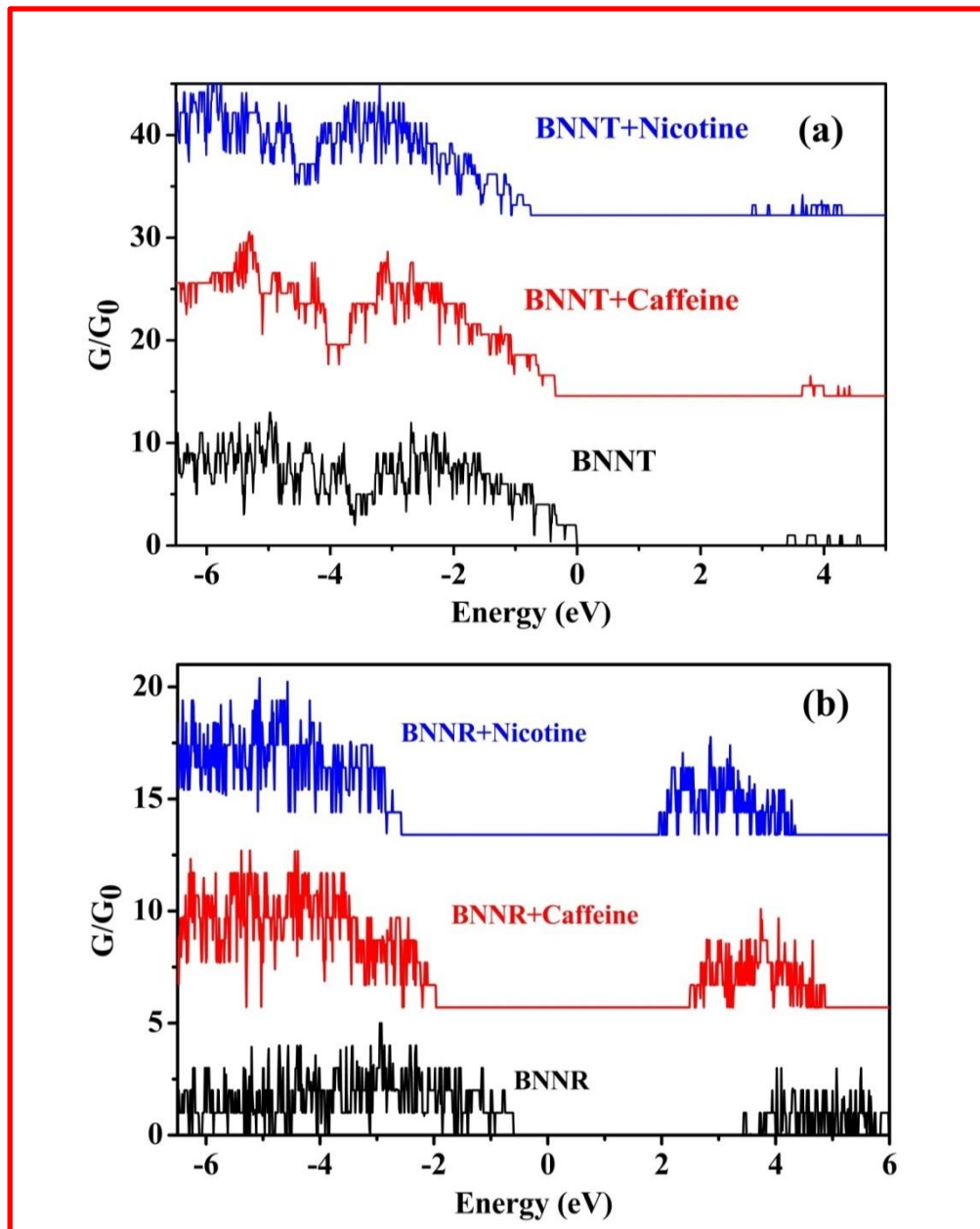


*Figure 3.8: Quantum conductance plot of BNNT and BNNR (a) conjugated with Nicotine and (b) conjugated with Caffeine.*

To judge the modification in the electronic conductance of a host adsorbate after adsorption of a molecule, we have calculated the quantum conductance to study the quantum transport of charge. Furthermore, the quantum conductance confirms the behavior of electronic

DOS and helps in understanding the possible charge transfer. The calculated quantum conductance for pristine and alkaloids adsorbed BNNT and BNNR is shown in Fig. 3.8. The sharp Van – Hove singularity in the density of states can be clearly seen in the calculated quantum conductance which has a typical step by step like behavior. The significant change in the conductance of BNNs after adsorption is attributed to the different electronic DOS at the Fermi level for BNNs, caffeine and nicotine. The conductance plot of alkaloids adsorbed BNNs are close to the superposition of that of a considered pristine BNNs conductance which can be seen from Figs. 3.8 (a-b). Thus it supports the conclusion which is drawn from DOS of adsorbed molecule system, that there is no significant charge transfer between BNNs and alkaloids. However, a significant shift in peaks is observed in comparison to pristine BNNT and BNNR. The shift is more prominent in case of nicotine which suggests that the BNNs can sense nicotine better compared to caffeine and also clearly distinguish each other. Similar conclusion is drawn for the sulphur chain encapsulated inside CNT [56-57]. Thus, our conductance calculations suggest that the caffeine and nicotine molecules modify the electronic conductance of BNNT and BNNR which provide solid support for new conduction channels in the adsorbed biomolecule BN system.

### **3.4 Conclusions**

Caffeine and nicotine being stimulants for central nervous system are highly addictive drugs that will lead to high blood pressure, insomnia etc. in humans if not consumed in proper dosage. Accordingly, the manufacturing of nanostructure sensors and filters to capture these alkaloids are in development. Present study shows the interaction mechanism of boron nitride

nanostructures, namely BNNT and BNNR with two different alkaloids caffeine and nicotine for their sensing application using dispersion-corrected density functional theory. Our results on the geometric properties, adsorption energy, electronic structure, charge transfer and quantum conductance indicate that the caffeine and nicotine molecules strongly bind to BNNR and BNNT. However, the binding is strong for BNNR than BNNT. The incorporation of dispersion correction enhances the adsorption strength of these molecules with BNNR and BNNT. Negligible charge transfer is observed between the considered alkaloids and BNNT/BNNR. The caffeine molecule shows the strong binding with both nanostructures but binds more strongly with BNNR compared to nicotine. We observed that the adsorption of charge donor molecules modulates the electronic DOS. The investigation of DOS and PDOS clearly shows the localization at top of valence band that further depicts the contribution of alkaloids, caffeine and nicotine. We found that the electronic properties of BNNR are more sensitive to the presence of caffeine and nicotine, which indicates that BNNR is a promising candidate for the detection of these alkaloid molecules. Our results clearly reveal that the BNNR is an effective substrate for the non-covalently binding of alkaloid molecules. The conclusion of this study may motivate experimentalists to study these nanostructures for the applicability as sensors, carriers and filters.

## **References**

1. Y. F. Zhukovskii, S. Piskunov, J. Kazerovskis and D. V. Makaev, *J. Phys. Chem. C* **117**, 14235 (2013).
2. N.G. Chopra, R.J. Luyken, K. Cherrey, V.H. Crespi, M.L. Cohen, S.G. Louie and A. Zettl, *Science* **269**, 966 (1995).

3. X. Fua and R. Zhang, *Nanoscale*. **9**, 6734 (2017).
4. Y. Chen, J. Zou, S.J. Campbell, G. Le Caer, S.J. Campbell and G. L. Caer, *Appl. Phys. Lett.* **84**, 2430 (2004).
5. S. Kalay, Z. Yilmaz, O. Sen, M. Emanet and E. Kazanc, *Beilstein J. Nanotechnol.* **6**, 84 (2015).
6. S.D. Dabhi and P.K. Jha, *Mater. Res. Express.* **3**, 085015 (2016).
7. S. Trivedi, S. Kumar, S.C. Sharma and S.P. Harsha, *IET Nanobiotechnol.* **9**, 259 (2015).
8. B. Aksoy, A. Paşahan, Ö. Güngör and S. Köytepe, *Int. J. Polym. Mater. Polym. Biomater.* **66**, 203 (2017).
9. G. Ciofani, *Expert Opin Drug Deliv.* **7**, 889 (2010).
10. G. Ciofani and V. Mattoli, *Boron Nitride Nanotubes in Nanomedicine*, 1st ed; Elsevier Science & Technology Books: Netherlands, 2016. ISBN: 978-0-323-38945-7.
11. D. Golberg, Y. Bando, Y. Huang, T. Terao, M. Mitome and C. Tang, *ACS Nano*. **4**, 2979 (2010).
12. P. K. Jha and H. R. Soni, *J. Appl. Phys.* **115**, 023509 (2014).
13. A. Pakdel, C. Zhi, Y. Bando and D. Golberg, *Mater. Today* **15**, 256 (2012).
14. X. Chen, P. Wu, M. Rousseas, D. Okawa, Z. Gartner and A. Zettl, *J. Am. Chem. Soc.* **131**, 890 (2009).
15. Z. Zhang and W. Guo, *Phys. Rev. B* **77**, 075403 (2008).
16. Y. Zhang, X. Wu, Q. Li and J. Yang, *J. Phys. Chem. C*. **116**, 9356 (2012).
17. R. B. Chen, C.P. Chang, F.L. Shyu and M. F. Lin, *Solid State Commun.* **123**, 365 (2002).

18. K. Zhao, M. Zhao, Z. Wang and Y. Fan, *Phys. E.* **43**, 440 (2010).
19. R. M. Ribeiro and N.M.R. Peres, *Phys. Rev. B* **83**, 235312 (2011).
20. J. Nakamura, T. Nitta and A. Natori, *Phys. Rev. B* **72**, 205429 (2005).
21. A. J. Du, S. C. Smith and G.Q. Lu, *Chem. Phys. Lett.* **447**, 181 (2007).
22. C. K. Yang, *Comput. Phys. Commun.* **182**, 39 (2011).
23. D. Farmanzadeh and S. Ghazanfary, *Comptes Rendus - Chim.* **17**, 985 (2014).
24. E. C. Anot, Y. Tlapale, M. S. Villanueva, J. A. R. Márquez, *J Mol Model.* **21**, 215 (2015).
25. B. Cai, S. Zhang, Z. Yan and H. Zeng, *Chem Nano Mat*, **1**, 542 (2015).
26. Q. Weng, B. Wang, X. Wang, N. Hanagata, X. Li, D. Liu, X. Wang, X. Jiang, Y. Bando and D. Golberg, *ACS Nano.* **8**, 6123 (2014).
27. I. V. Sukhorukova, I. Y. Zhitnyak, A. M. Kovalskii, A. T. Matveev, O. I. Lebedev, X. Li, N. A. Gloushankova, D. Golberg and D.V. Shtansky, *ACS Appl. Mater. Interfaces*, **7**, 17217 (2015).
28. S. M. Chowdhury, G. Lalwani, K. Zheng, J. Y. Yang, K. Neville and B. Sitharaman, *Biomaterials* **34**, 283 (2013).
29. H. Zhang, G. Gruner and Y. Zhao, *J. Mater. Chem. B* **1**, 2542 (2013).
30. J. Rusted, L. Graupner, N. O'Connell and C. Nicholls, *Psychopharmacology* **115**, 547 (1994).
31. D. Bishop, *Sports Med.* **40**, 995 (2010).
32. D. Robertson, D. Wade, R. Workman, R. Woosley and J. A. Oates, *J. Clin Invest.* **67**, 1111 (1981).

33. Z. G. Chen, L. S. Zhang, Y. W. Tang and Z. J. Jia, *Appl. Surf. Sci.* **252**, 2933 (2006).
34. E.C. Girão, S.B. Fagan, I. Zanella and A.G. Souza, *J. Hazard. Mater.* **184**, 678 (2010).
35. H. J. Lee, G. Kim and Y. K. Kwon, *Chem. Phys. Lett.* **580**, 57 (2013).
36. J. Wang, V.K. Kayastha, Y.K. Yap, Z. Fan, J.G. Lu, Z. Pan, I.N. Ivanov, A.A. Puretzky and D.B. Geohegan, *NanoLett.* **5**, 2528 (2005).
37. L.H. Li, J. Cervenka, K. Watanabe, T. Taniguchi and Y. Chen, *ACS Nano.* **8**, 1457 (2014).
38. C.Y. Zhi, Y. Bando, C.C. Tang, Q. Huang and D. Golberg, *J. Mater. Chem.* **18**, 3900 (2008).
39. A. Soltani, M.T. Baei, E.T. Lemeski and M. Shahini, *Superlattice. Microstruct.* **76**, 315 (2014).
40. M. T. Baei, *Comput. Theor. Chem.* **1024**, 28 (2013).
41. M. D. Esrafil and R. Nurazar, *Superlattice. Microstruct.* **67**, 54 (2014).
42. S. Mukhopadhyay, R.H. Scheicher, R. Pandey and S.P. Karna, *J. Phys. Chem. Lett.* **2**, 2442 (2011).
43. X. Zhong, S. Mukhopadhyay, S. Gowtham, R. Pandey and S.P. Karna, *Appl. Phys. Lett.* **102**, 133705 (2013).
44. P. Giannozzi et al., *J. Phys. Condens. Matter.* **21**, 395502 (2009)
45. J. P. Perdew, K. Burke and M. Ernzerhof, *Phys. Rev. Lett.* **77**, 3865 (1996).
46. H. J. Monkhorst and J.D. Pack, *Phys. Rev. B.* **13**, 5188 (1976).
47. B. Civalleri, L. Maschio, P. Ugliengo and C. M. Z Wilson, *Phys. Chem. Chem. Phys.* **12**, 6382 (2010).

48. S. Grimme, *J. Comput. Chem.* **27**, 1787 (2006).
49. R. Landauer, *Philos. Mag.* **21**, 863 (2016).
50. A. A. Mostofi, J. R. Yates, Y. Lee, I. Souza, D. Vanderbilt and N. Marzari, *Comput. Phys. Commun.* **178**, 685 (2008).
51. O. Kwon and M.L. Mckee, *J. Phys. Chem. A.* **104**, 7106 (2000).
52. H. Yildirim, T. Greber and A. Kara, *J. Phys. Chem. C.* **117**, 20572 (2013).
53. L. Debbichi, Y. J. Dappe and M. Alouani, *Phys. Rev. B* **85**, 045437 (2012).
54. S. Mukhopadhyay, S. Gowtham and R.H. Scheicher, *Nanotechnology.* **21**, 165703 (2010).
55. R. Tadmor, *J. Phys. Condens. Matter.* **13**, 195 (2001).
56. A. Calvi, A. Ferrari, L. Sbuelz, A. Goldoni and S. Modesti, *Sensors.* **16**, 731 (2016).
57. T. Fujimori, A. M. Gomez, Z. Zhu, H. Muramatsu, R. Futamura, K. Urita, , M. Terrones, T. Hayashi, M. Endo, S. Y. Hong, Y. C. Choi, D. Toma and K. Kaneko, *Nat. Commun.* **4**, 2162 (2013).